Engineering the Redox Potential over a Wide Range within a New Class of FeS Proteins

John A. Zuris[†], Danny A. Halim[†], Andrea R. Conlan[†], Edward C. Abresch[‡], Rachel Nechushtai[§], Mark L. Paddock[‡], Patricia A. Jennings*[,†]

[†]Department of Chemistry and Biochemistry and [‡]Department of Physics, University of California at San Diego, La Jolla, CA 92093. [§]Department of Plant and Environmental Sciences, The Wolfson Centre for Applied Structural Biology, The Hebrew University of Jerusalem, Givat Ram, Israel 91904

Supporting Information

Materials and Methods

Protein Expression and Purification: Over-expression and purification of mitoNEET proteins were performed as outlined.[S1]

Optical Spectroscopy and pH Titrations: All UV-Visible absorption spectra were measured from the near UV to the near IR (300 - 700 nm) on a Cary50 spectrometer (Varian Inc, Palo Alto CA) equipped with a temperature-controlled cell (T = 25°C) (50-100 μM protein in 25 mM Tris-HCl, 100 mM NaCl, pH 8 buffer). The p*K(ox)* of His87 when the [2Fe-2S] centers are in the oxidized state was determined by monitoring the shift in the wavelength peak position as a function of pH:

$$\lambda_{obs} = \lambda_{unprot} + \Delta\lambda / [1 + 10^{(pH - pK(ox))}] \qquad \text{(Eq. S1)}$$

where λ_{obs} is the observed maximum peak value near 458 nm at a given pH for the species under investigation, λ_{unprot} is the wavelength peak when His87 is deprotonated, and $\Delta\lambda$ is the difference between the wavelength of the fully protonated species and the fully unprotonated species. The pK_a (red) of His87 when the [2Fe-2S] centers are in the reduced state was determined similarly using the equation below:

$$\lambda_{obs} = \lambda_{unprot,\,red} + \Delta\lambda / [1 + 10^{(pH - pK(red))}] \qquad \text{(Eq. S2)}$$

where $\lambda_{unprot,\,red}$ is 546 nm (for WT) or 544 nm (for K55E) and represents the reduced peak that undergoes a shift at high pH. As in Eq. S1, λ_{obs} , $\Delta\lambda$, and pH are the observed wavelength, the difference in peak wavelength (546 nm vs. 553 nm) between the pH extremes, and the $[H^+]$, respectively. For more information see reference S2.

Optical Redox Titrations: A detailed explanation of optical titration methods can be found in Dutton *et al.* (1978).[S3] The reduction state was determined by monitoring the absorbance at 458 nm with 100 μM mitoNEET for both WT and mutants under appropriate buffer conditions, depending on pH. The ambient redox potential was adjusted by adding dithionite and measured with a Ag/AgCl dual reference and working electrode (Microelectrodes Inc, Bedford NH), and potentials were adjusted to Standard Hydrogen Electrode (SHE) values for presentation. The accuracy of the Ag/AgCl electrode was checked after each experiment using a set of quinone/quinhydrone standards (Sigma-Aldrich) as recommended by the manufacturer. An elixir of redox mediators was used to ensure equilibration and stability. All mediators were purchased from Sigma-Aldrich and were chosen to span the potential region of both the WT protein and the mutants in this study. The mediators employed and their respective concentrations were: 1,4-benzoquinone (50 μM), methylene blue (25 μM), menadione (50 μM), 1,4-naphthoquinone (25 μM), anthraquinone-2-sulfonate (25 μM), dithiothreitol (50 μM), and methyl viologen (2 μM). Absorbance values at 458 nm were converted to fraction oxidized, in which the fully oxidized 458 nm peak corresponded to 1.0 and the fully reduced 458 nm peak corresponded to 0.0. The equation is given below:

$$\text{Fraction Oxidized} = (A_{obs} - A_{red}) / (A_{ox} - A_{red}) \qquad \text{(Eq. S3)}$$

where A_{obs} is the measured absorbance at a given potential, A_{red} is the absorbance of the fully reduced sample, and A_{ox} is the absorbance of the fully oxidized sample. Origin 6.1 (OriginLab Corporation) was used to determine the midpoint/redox potential (E_M) from a fit of the fraction oxidized versus potential using the Nernst equation below:

$$\text{Fraction Oxidized} = 1/\{1 + 10^{[(E_M\text{-E})*n/59.1\ \text{mV})]}\} \qquad \text{(Eq. S4)}$$

where E_M is the redox midpoint potential of the species, E is the ambient cell potential corresponding to each fraction oxidized, and n is the number of electrons in the chemical reaction. Optical redox titration data was fit to a pK_a using the equation below:

$$E_M = E_{acid} + 2.303(RT/nF)*\log\{([H^+] + K_a^{red})/([H^+] + K_a^{ox})\} + \alpha(pH) \quad \text{(Eq. S5)}$$

where E_M is the measured redox potential of the species under study, E_{acid} is the redox potential limit at low pH, R is the universal gas constant, T is temperature measured in K, n is the number of electrons involved in the chemical reaction, F is Faraday's constant, $[H^+]$ is the concentration of protons in solution, and K_a^{ox} and K_a^{red} are the proton equilibrium constants for the oxidative reaction and reductive reaction, respectively. We also introduce α(pH) as a global factor to account for all pH-dependent changes from pH 6 to 11 other than titration of His87, which is explicitly treated. To first order we have treated α(pH) as α*pH. It introduces an overall decrease in magnitude of the slope that amounts to ~15%. For the H87C mutant, there is no His87 titration and so the equation reduces to $E_M = E_{acid} + \alpha(pH)$, with α accounting for the shallow pH dependence that is observed in Fig. 3B. Units for the E_M are reported in millivolts (mV).

Protein-film voltammetry: A detailed description of protein-film voltammetry can be attained from previous work.[S4] Protein-film voltammograms were generated using a CHI 730C Electrochemical Workstation (CH Instruments Inc., Austin TX) equipped with an in-house glass electrochemical cell supporting a working electrode, a 3 M Ag/AgCl reference electrode, and platinum wire counter electrode. The working electrode was purchased from ALS (Tokyo, JP) and was comprised of highly oriented edge-plane graphite (HOPG) with a surface area of 7 mm^2. Preparation of protein films and the choice of buffers for different pH measurements were performed as reported previously.[S5] The glass cell and the sample buffer were chilled in a water bath set to 4 °C. Scan rates were performed at 200 mV/s as reported previously [S5] over a range from +0.5 V to -0.6 V vs. SHE. No changes in E_M outside of the normal uncertainty (± 5 mV) in measurements were observed over scan rates from 50 mV/s to 400 mV/s. No appreciable shifts (± 5 mV) in redox potential were observed in the WT by going to either higher salt concentrations (1 M) or switching to different buffers. All measurements were taken at 4 °C to enhance the amplitude of the anodic and cathodic peak potentials[S4], and spot checking measurements at 25 °C showed the same results within uncertainty (±

5 mV).[S5] Baseline subtraction of voltammetry data was performed using the SOAS software package, courtesy of Christopher Leger.[S6] All data were obtained using the Ag/AgCl reference electrode (+205 mV SHE) and checked for accuracy using methylene blue (Sigma-Aldrich) as a standard. Measurements were corrected to SHE for presentation.

A systematic shift of -25 ± 4 mV was observed for PFV compared to the optical method. The E_M for D84G at pH 6.0 was measured using PFV and was shifted by + 25 mV for comparison with the optical redox titration E_M values shown in Figure 1.

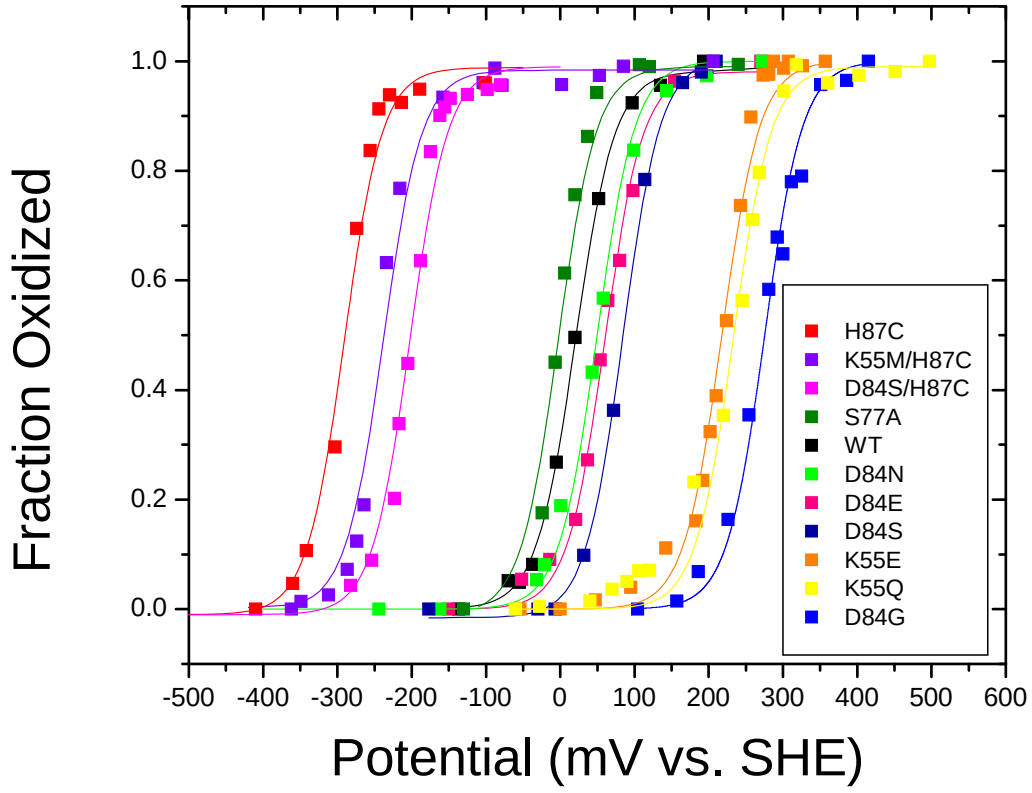

Figure S1. Measurements and fit of optical titration data of WT mitoNEET and several mutants at pH 7.0. All samples were measured in 100 mM Bis-Tris pH 7.0. Data were fit to a Nernstian curve (Equation S4). $E_{M,7}$ values of each mitoNEET mutant, in order from left to right, are as follows: H87C (-290 mV), K55M/H87C (-270 mV), D84S/H87C (-210 mV), S77A (-2 mV), WT (+25 mV), D84N (+48 mV), D84E (+66 mV), D84S (+90 mV), K55E (+185 mV), K55Q (+200 mV), D84G (+270 mV).

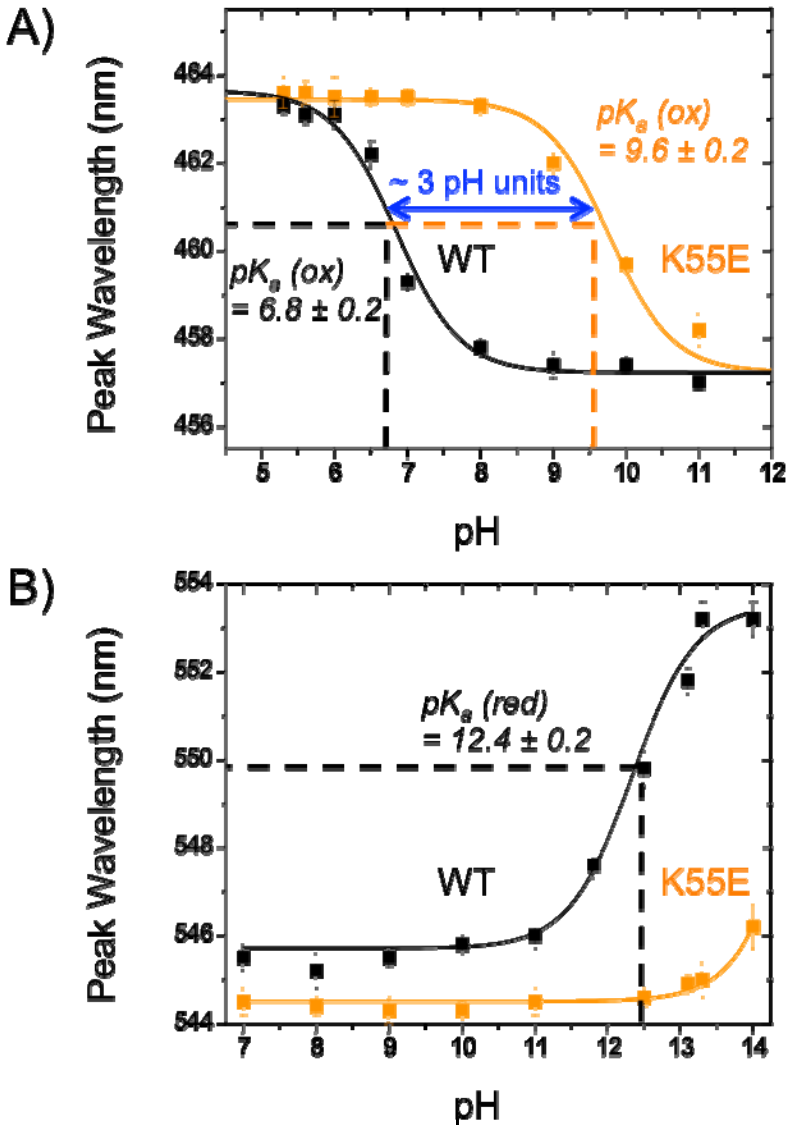

Figure S2. A) Optical pH titration shifts for WT mitoNEET (black squares) and the K55E mutant (orange squares) in the oxidized state. Data were fitted to a pH titration equation (Equation S1) and showed a single titration from pH 5 to 14. Spectra indicate that the p*K(ox)* of Nε on His87 shifts from 6.8 ± 0.2 in the WT to 9.6 ± 0.2 in the K55E mutant. Peak wavelength values at 463 nm correspond to protonated His87, whereas those at 457 nm correspond to deprotonated His87. B) Optical pH titration shifts for WT and the K55E mutant in the reduced state fit with Eq. S2. The p*K(red)* for His87 in the WT in was determined to be 12.4 ± 0.2. The H87C mutant showed no shifts in either state, confirming the assignment of the single titrating group to His87.

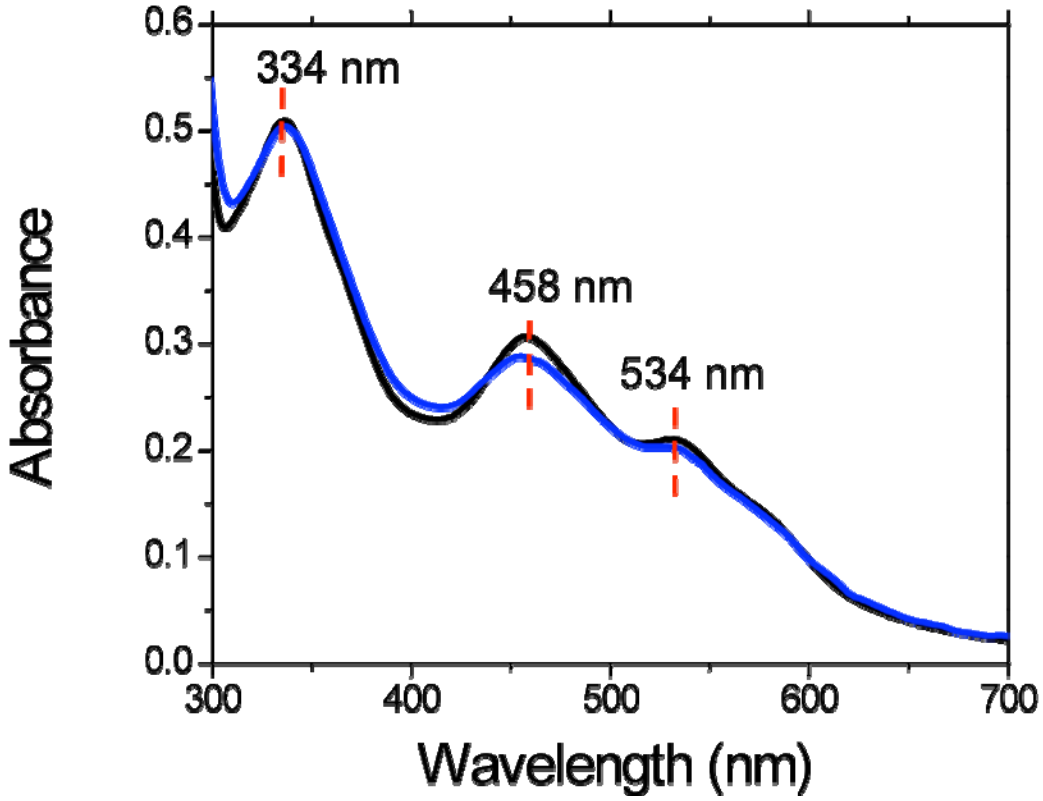

Figure S3. Optical Spectra of WT MitoNEET (black) and the D84G (blue) mutant at pH 8.0. Samples were measured in 50 mM Tris 100 mM NaCl. Optical spectra indicate similar coordination geometries for the WT and D84G as the signature peak at 458 nm appear to be similar in both species. Peaks at 334 nm and 534 nm are also very similar. In contrast, the H87C mutant displays large changes at the 458 nm peak, with a significant shoulder appearing near 420 nm as previously reported.[S7]

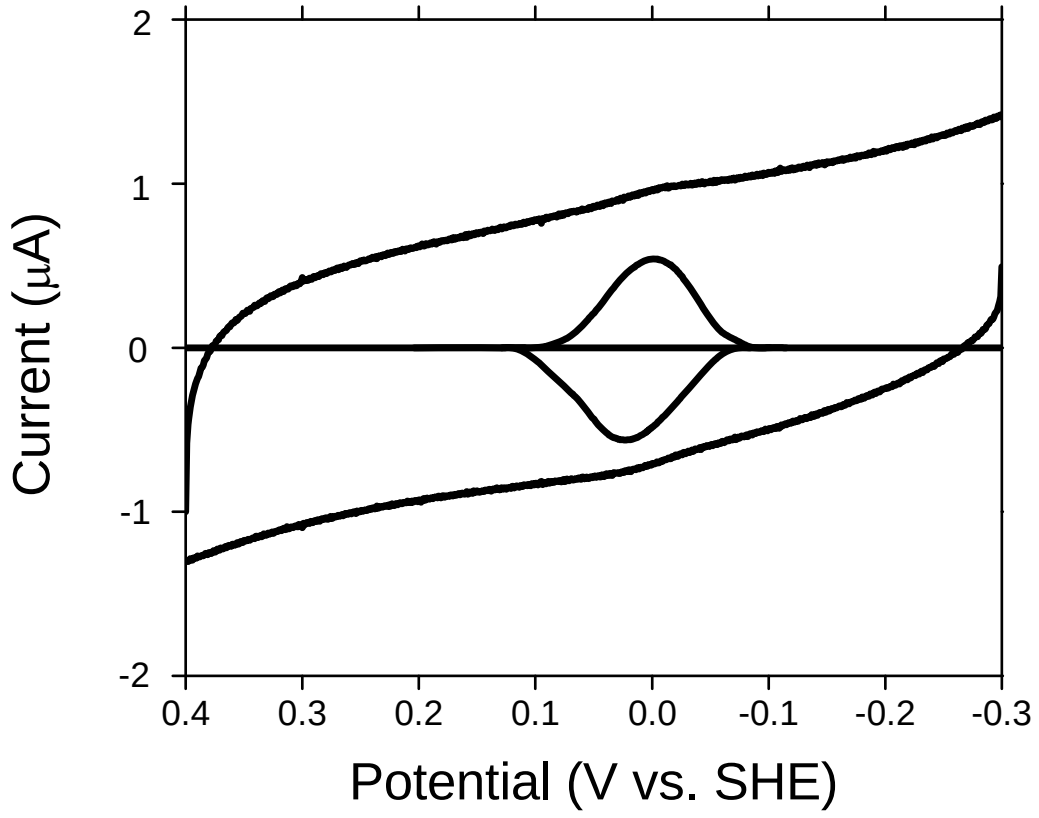

Figure S4A. Outset) Protein-film voltamogram of WT MitoNEET, pH 7.0. Inset) Baseline subtracted anodic and cathodic peaks (not shown to scale).

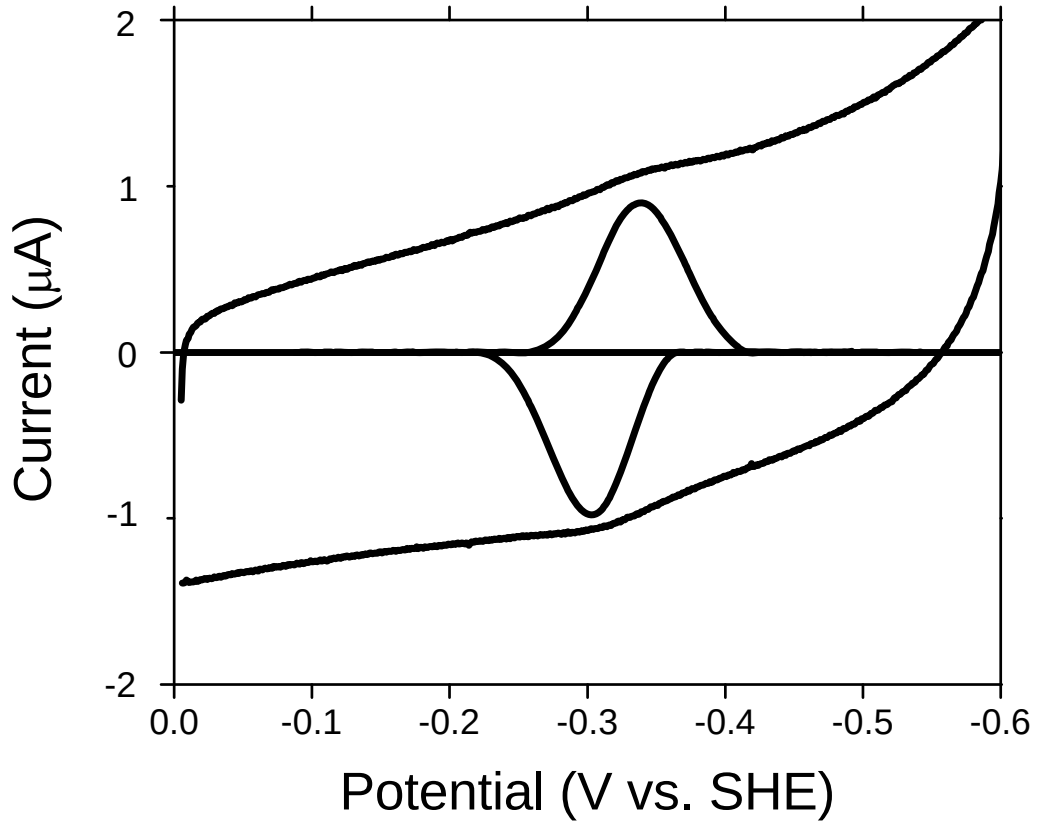

Figure S4B. Outset) Protein-film voltammogram of H87C, pH 7.0. Inset) Baseline subtracted anodic and cathodic peaks (not shown to scale).

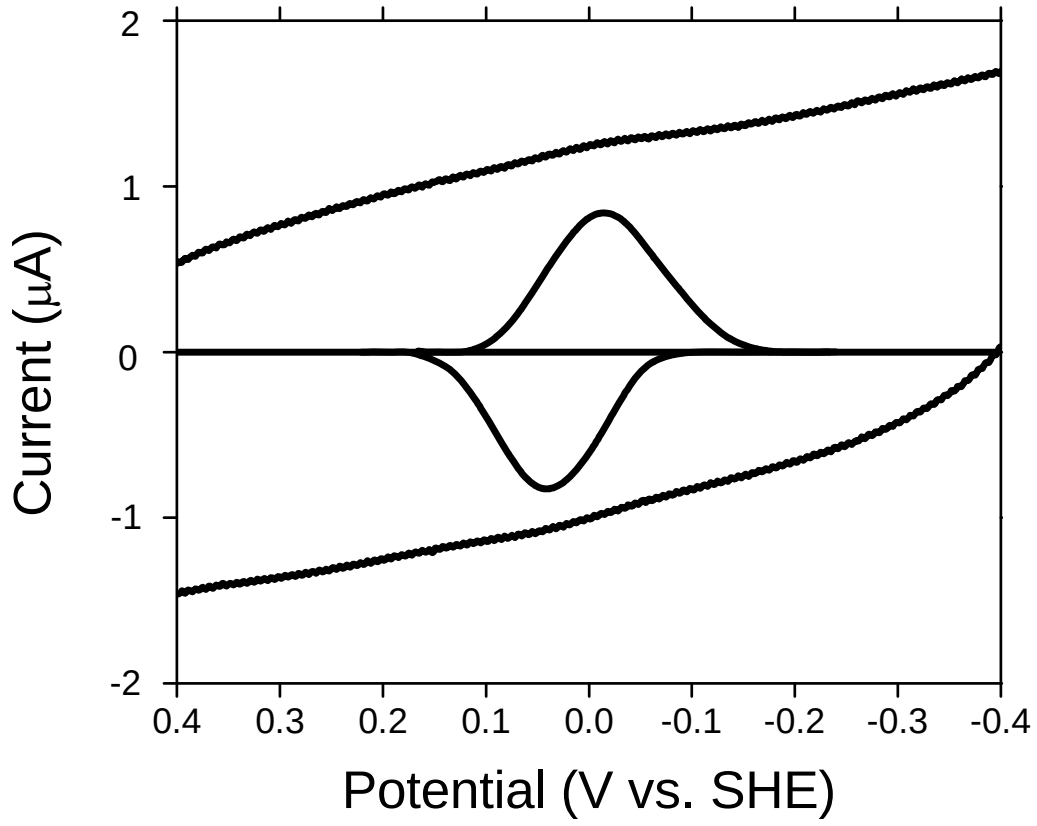

Figure S4C. Outset) Protein-film voltammogram of D84N, pH 7.0. Inset) Baseline subtracted anodic and cathodic peaks (not shown to scale).

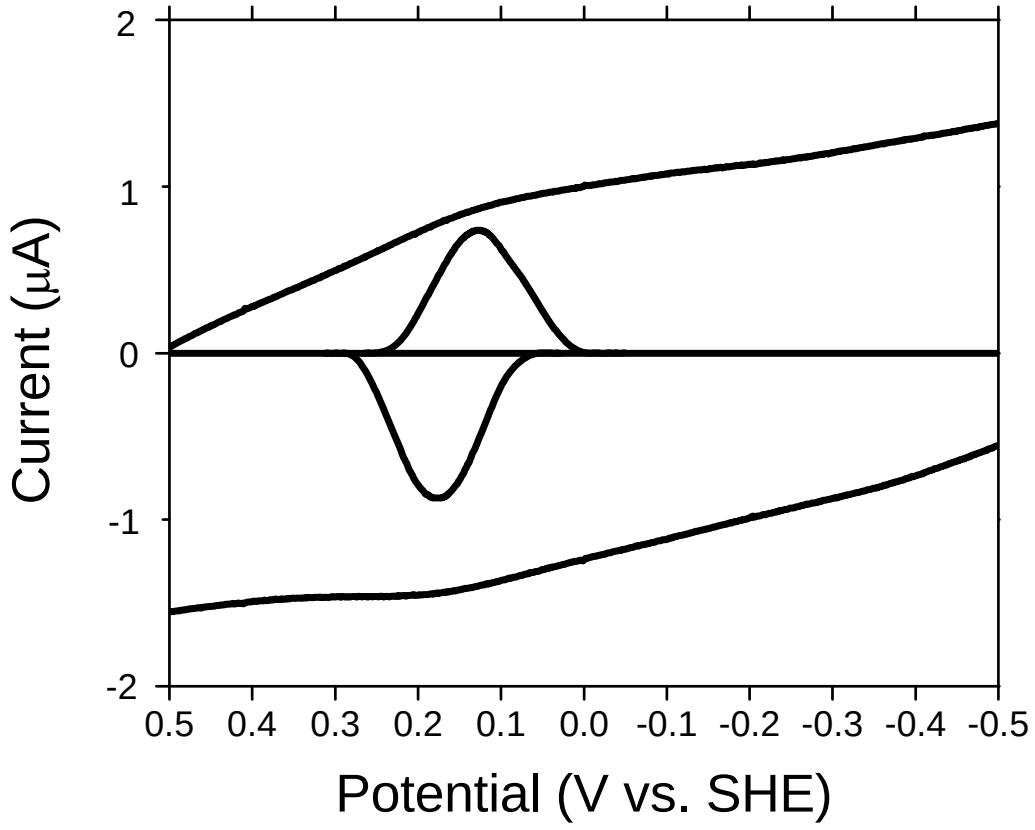

Figure S4D. Outset) Protein-film voltammogram of K55E, pH 7.0. Inset) Baseline subtracted anodic and cathodic peaks (not shown to scale).

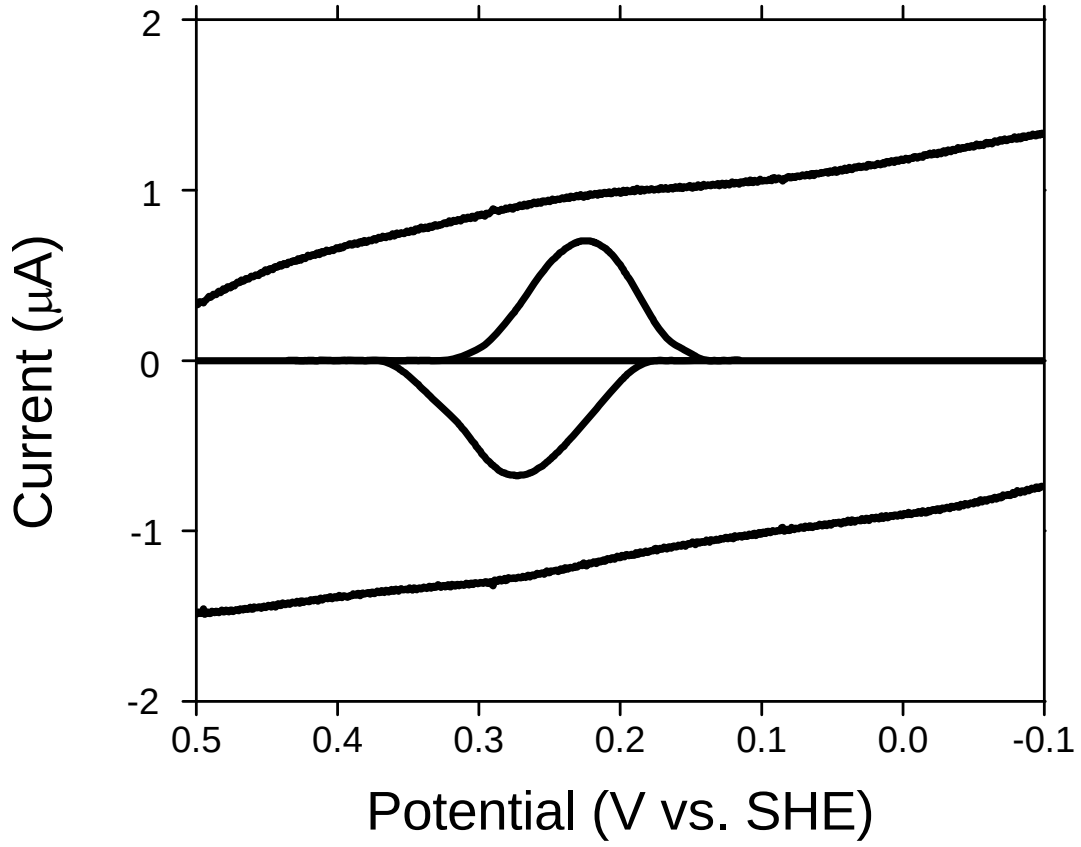

Figure S4E. Outset) Protein-film voltammogram of D84G, pH 7.0. Inset) Baseline subtracted anodic and cathodic peaks (not shown to scale).

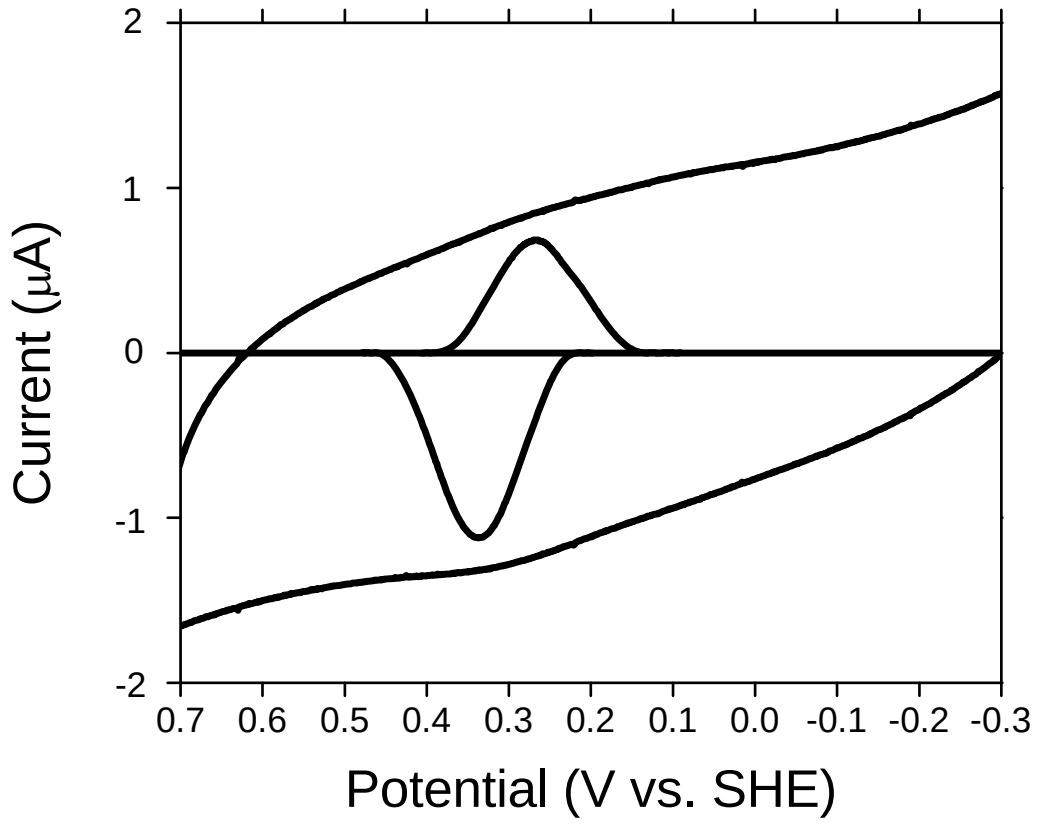

Figure S4F. Outset) Protein-film voltammogram of D84G, pH 6.0. Inset) Baseline subtracted anodic and cathodic peaks (not shown to scale).

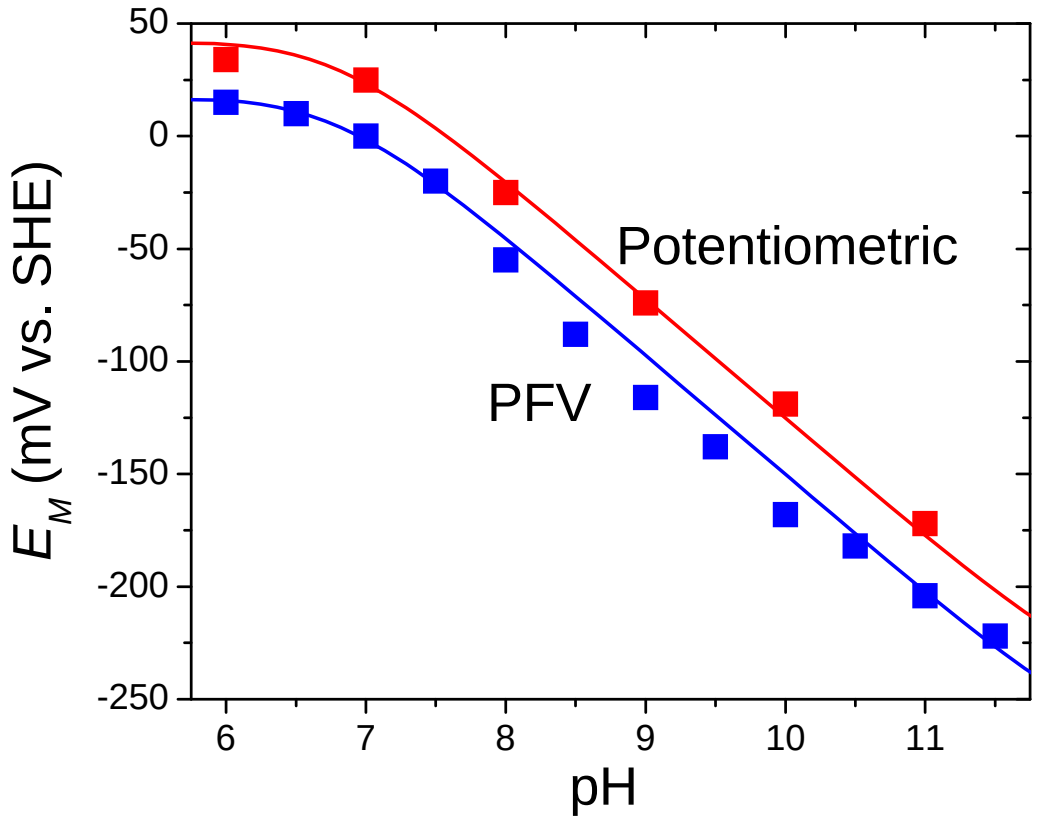

Figure S5. Redox potentials for WT MitoNEET as a function of pH measured using potentiometric titrations (red squares) and protein-film voltammetry (blue squares). Data were fit using Eq. S5 with pK_{ox} = 6.7 ± 0.2 and pK_{red} fixed at 12.4 based on the optical titration data (Fig. S2B). Data show a 25 mV offset between the two techniques that appears to be approximately constant across the pH range. PFV and potentiometric titration data agree well with previously reported data for WT mitoNEET[S5]

Table S1. Redox Potentials of MitoNEET and mutants

MitoNEET Mutant	$E_{M,7}{}^{Opt}$ (mV)	$E_{M,7}{}^{PFV}$ (mV)
WT	+25[a]	0[b]
K55E	+185	+166
K55Q	+200	+176
S77A	-2	n.a.
D84E	+66	n.a.
D84G	+270	+255
D84N	+48	+19
D84S	+90	n.a.
H87C	-290[b]	-320[b]
K55M/H87C	-270	n.a.
D84S/H87C	-210	n.a.

Redox measurements performed by optical titrations methods and spot checked by PFV with $E_{M,7}$ values for both techniques shown. WT and different mutants are shown in order of residue number with double mutants shown last. A systematic shift ($E_M{}^{Opt}$ – $E_M{}^{PFV}$) of 25 ± 4 mV was observed for the two methods. This systematic shift matches previous reports[S5] and is the same at 25 ˚C and 4 ˚C, and thus is not attributable to temperature effects. Errors for both optical and PFV measurements were estimated to be around ± 10 mV. [a]These values agree with previously reported values.[S1] [b]These values agree with previously reported values.[S5]

Supporting References

(S1) Conlan, A. R.; Axelrod, H. L.; Cohen, A. E.; Abresch, E. C.; Zuris, J. A.; Yee, D.; Nechushtai, R.; Jennings, P. A.; Paddock, M. L. *J. Mol. Biol.* **2009** *392*, 143–153.

(S2) Kuila, D.; Fee, J. A. *J. Biol. Chem.* **1986** *261*, 2768-2771.

(S3) Dutton, P. L. *Methods Enzymol.* **1978** *54*, 411–435.

(S4) Armstrong, F. A.; Butt, J. N.; A. Sucheta, A. *Methods Enzymol.* **1993** *227*, 479-500

(S5) Bak, D. W.; Zuris, J. A.; Paddock, M. L.; Jennings, P. A.; Elliott, S. J. *Biochemistry* **2009** *48*, 10193–10195.

(S6) Fourmond, V.; Hoke, K.; Heering H. A.; Baffert, C.; Leroux, F.; Bertrand, P.; Léger, C. *Bioelectrochemistry* **2009** *76*, 141-147.

(S7) Wiley, S. E.; Paddock, M. L.; Abresch, E. C.; Gross, L.; van der Geer, P.; Nechushtai, R.; Murphy, A. N.; Jennings, P. A.; Dixon, J. E. *J. Biol. Chem.* **2007** *282*, 23745-23749.